
Article:
Cockram, A.A., Bradley, R.D., Lynch, S.A. et al. (5 more authors) (2018) Optimization of the high-throughput synthesis of multiblock copolymer nanoparticles in aqueous media: Via polymerization-induced self-assembly. Reaction Chemistry and Engineering, 3 (5). pp. 645-657.

https://doi.org/10.1039/c8re00066b

Optimization of the high-throughput synthesis of multiblock copolymer nanoparticles in aqueous media via polymerization-induced self-assembly

Amy A. Cockram[†], Robert D. Bradley[‡], Sylvie A. Lynch[‡], Patricia C. D. Fleming[‡], Neal S. J. Williams[‡], Martin W. Murray[‡], Simon N. Emmett[‡], Steven P. Armes[*†]

[†]Dainton Building, Department of Chemistry, The University of Sheffield, Brook Hill, Sheffield, South Yorkshire S3 7HF, UK.

[‡]AkzoNobel Decorative Paints, Wexham Road, Slough, Berkshire SL2 5DS, UK.

Abstract. Over the past fifteen years or so, polymerization-induced self-assembly (PISA) has become widely recognized as a powerful and versatile platform technology for the synthesis of a wide range of block copolymer nanoparticles of controlled size, shape and surface chemistry. In the present study, we report that PISA formulations are sufficiently robust to enable high throughput experiments using a commercial synthesis robot (Chemspeed Autoplant A100). More specifically, we use reversible addition-fragmentation chain transfer (RAFT) aqueous emulsion polymerization of either n-butyl methacrylate and/or benzyl methacrylate to prepare various examples of methacrylic multiblock copolymer nanoparticles using a poly(methacrylic acid) stabilizer block. Adequate stirring is essential to generate sufficiently small monomer droplets for such heterogeneous polymerizations to proceed efficiently. Good reproducibility can be achieved under such conditions, with well-defined spherical morphologies at up to 45 % w/w solids. GPC studies indicate high blocking efficiencies but relatively broad molecular weight distributions (M_w/M_n = 1.36-1.85), suggesting well-defined (albeit rather polydisperse) block copolymers. These preliminary studies provide a sound basis for high-throughput screening of RAFT-mediated PISA formulations, which is likely to be required for commercialization of this technology. Our results indicate that such PISA formulations enable the synthesis of diblock and triblock copolymer nanoparticles in high overall yield (94-99%) within 1-3 h at 70 °C. However, tetrablocks suffer from incomplete conversions (87-96% within 5 h) and hence most likely represent the upper limit for this approach.

Introduction

Reversible addition-fragmentation chain transfer (RAFT) polymerization is a widely-used technique in the field of controlled radical polymerization.[1, 2] In recent years, its use has increased significantly, not least because it affords the ability to synthesize well-defined, low-

polydispersity block copolymers ($M_w/M_n \leq 1.20$) using a wide range of functional vinyl monomers. Moreover, RAFT polymerizations can be conducted in aqueous media,[3] which is highly attractive from both a commercial and environmental viewpoint. Originally, the main focus was on RAFT aqueous solution polymerization,[4-9] but more recently there has been greater emphasis on RAFT aqueous emulsion polymerization[10-28] (using water-immiscible monomers such as styrene, methyl methacrylate or n-butyl acrylate) and RAFT aqueous dispersion polymerization[29-43] (using water-miscible monomers such as 2-hydroxypropyl methacrylate). Such formulations can be used to synthesize a remarkably wide range of block copolymer nanoparticles via polymerization-induced self-assembly (PISA)[16, 31, 32, 36, 41-49] PISA enables the rational synthesis of diblock copolymer nanoparticles directly in water at relatively high concentrations (≤ 50 % w/w).[41, 50] Various block copolymer morphologies (e.g. spheres[25, 31, 51], worms[52], nanofibers,[16] vesicles[31, 53], framboidal vesicles[38], monkey nuts[28], jellyfish[32] and lamellae[43]) can be obtained, often simply by varying the mean degree of polymerization (DP) of the respective blocks.[36, 42, 43, 45] In principle, such nanoparticles offer a wide range of potential applications, including use as flocculants[54], novel hydrogels[55], Pickering emulsifiers[56, 57] and coatings[58, 59].

Many important properties of the final block copolymer nanoparticles can be readily tuned by choosing appropriate monomers, targeting suitable block DPs and adjusting the block order.[18, 33, 36, 38, 44] Additional synthesis parameters such as copolymer concentration, solution pH, polymerization temperature, reaction time, and RAFT agent/initiator molar ratio can also play important roles in determining a successful outcome for a given PISA synthesis.[17, 23, 25, 36, 43] Given this complexity, optimization of new PISA formulations can be a time-consuming and laborious task, particularly if the construction of phase diagrams is desired.[36, 41, 42, 60, 61] In principle, this 'bottleneck' problem can be addressed by using a high-throughput strategy to perform parallel syntheses of multiple reactions under similar conditions.[62-64] For example, the Chemspeed Autoplant A100 automated synthesizer (Figure 1) can perform up to twenty parallel syntheses, which enables several parameters to be explored simultaneously. This high-throughput approach has been successfully applied in many fields such as the pharmaceutical industry, materials research, and polymer science.[62, 63, 65-74] For example, pharmaceutical research has benefited from rapid screening of large libraries of potential lead compounds, which can cause a considerable reduction in time-to-market for novel drugs.[63, 65, 66] In the case of materials research,[67] high-throughput strategies have aided the discovery of novel superconducting materials[68], inorganic phosphorous compounds for use in flat-panel displays, lighting and x-ray imaging [69-72] and new polymer catalysts.[73-76] Of particular relevance to the

present study are high-throughput studies based on living radical polymerization.[77-81] For example, a library of acrylic diblock copolymers was synthesized using the so-called macromolecular design via the interchange of xanthates (MADIX) process.[77] The RAFT solution polymerization of methyl methacrylate in toluene was successfully transferred to an automated synthesizer (Chemspeed Accelerator^{TM} SLT00) to produce a series of well-defined homopolymers.[78] Such precursors were subsequently chain-extended in turn with various methacrylic comonomers to generate a range of well-defined AB diblock copolymers.[79] Similarly, Hoogenboom and co-workers chain-extended poly(methyl acrylate), poly(n-butyl acrylate), poly(methyl methacrylate) or poly(2-(dimethylamino)ethyl methacrylate) in turn with 1-ethoxyethyl acrylate using the same equipment.[80] The same team reported a standard protocol for the parallel optimization of RAFT polymerizations.[81] This body of prior work indicates that RAFT polymerizations are amenable to a high-throughput approach. However, as far as we are aware, high-throughput RAFT polymerizations have not yet been performed in water. Moreover, there appears to be no reports of the high-throughput synthesis of diblock copolymer nanoparticles via RAFT-mediated PISA. In principle, coupling RAFT aqueous emulsion polymerization with a high-throughput approach should enable the rapid, convenient synthesis of a library of block copolymer nanoparticles. However, in addition to standard deoxygenation protocols for these air-sensitive polymerizations, it is noteworthy that such heterogeneous formulations require adequate stirring to ensure the formation of sufficiently small monomer droplets for the efficient production of colloidally stable dispersions.[82] Herein we demonstrate that successful PISA syntheses can be performed with good reproducibility using a Chemspeed Autoplant A100, which is a commercial high-throughput robot synthesizer (see Figure 1). More specifically, the RAFT aqueous emulsion polymerization of benzyl methacrylate (BzMA) or n-butyl methacrylate (BMA) is conducted using a water-soluble poly(methacrylic acid) (PMAA) chain-transfer agent to generate a series of sterically-stabilized diblock, triblock and tetrablock copolymer nanoparticles at up to 45 % w/w solids.

Experimental Section

Materials. Methacrylic acid (MAA, 99 %), benzyl methacrylate (BzMA, 96 %), n-butyl methacrylate (BMA, 99 %) and 4,4′-azobis(4-cyanovaleric acid) (ACVA, ≥ 98 %), THF (HPLC, ≥ 99.9 %) and glacial acetic acid (≥ 99.85 %) were purchased from Sigma-Aldrich (UK) and used as received. The 4-cyano-4-(2-phenylethanesulfanylthiocarbonyl)sulfanyl-pentanoic acid (PETTC) RAFT agent was prepared as described previously.[83] The d_4-methanol

and d_8-tetrahydrofuran used for ^{1}H NMR studies were purchased from Goss Scientific Instruments Ltd. (Cheshire, UK). All other solvents were purchased from Sigma-Aldrich (UK) or VWR Chemicals (UK) and used as received. Deionized water was used in all experiments.

Synthesis of Poly(methacrylic acid) (PMAA) Macro-CTA at 40 % w/w solids. PETTC RAFT agent (21.77 g, 0.064 mol), MAA (230 g, 2.67 mol, target DP 50) and absolute ethanol (≥ 99.5 %, 376.7 g, 40 % w/w) were weighed into a 1 L round-bottom flask. The flask was covered with a five-necked lid and fitted with a condenser, overhead anchor-type stirrer, N_2 inlet and temperature probe. In a separate vial, ACVA (3.00 g, 10 mmol; CTA/initiator molar ratio = 5.0) was dissolved in a small volume of ethanol (~10 mL). Both reaction mixtures were degassed with nitrogen for 90 min while stirring at room temperature. After 90 min, the initiator solution was injected into the round-bottom flask under a N_2 atmosphere using a syringe. The reaction mixture was further degassed for 20 min before being heated at 70 °C by immersion in a pre-heated water bath. After 3 h, the flask was removed from the water bath, allowed to cool, and its contents were exposed to air to quench the polymerization. The resulting PMAA macro-CTA was then purified by precipitation into a five-fold excess of diethyl ether. The crude polymer was collected by filtration and redissolved in the minimum amount of ethanol, before a second precipitation into excess diethyl ether. The purified polymer was allowed to dry overnight before being redissolved in the minimum amount of water, followed by lyophilization. The mean degree of polymerization for this macro-CTA was calculated to be 56 by ^{1}H NMR (see, Figure S1). GPC analysis of methylated $PMAA_{56}$ macro-CTA (using THF eluent containing 4 % v/v glacial acetic acid, against poly(methyl methacrylate) standards) indicated M_n = 6,000 g mol^{-1} and M_w/M_n = 1.17, (see Figure 3).

Laboratory-Scale Synthesis of $PMAA_{56}$-$PBzMA_{500}$ Diblock Copolymer Nanoparticles at 20 % w/w Solids via RAFT Aqueous Emulsion Polymerization of Benzyl Methacrylate. A typical protocol for the synthesis of $PMAA_{56}$-$PBzMA_{500}$ nanoparticles was as follows: $PMAA_{56}$ macro-CTA (0.1171 g, 0.02 mmol), ACVA (0.0013 g; 0.05 mmol, macro-CTA/initiator molar ratio = 5.0) and water (8.47 g, 20 % w/w) were weighed into a 15 mL vial. The solution pH was adjusted to pH 5 using 1 M NaOH and BzMA monomer (2.00 g, 0.01 mol) was then added. The final mass of liquid reagents was ~10-11 g. A magnetic flea was added and the reaction vial was sealed using a rubber septum. The reaction solution was purged under N_2 for 15 min and the vial was then placed in a pre-heated water bath at 70 °C for 2 h, prior to its removal and exposure to air to quench the polymerization. In all the laboratory experiments, magnetic stirring was conducted at 500 rpm.

Laboratory-Scale One-Pot Synthesis of Tetrablock Copolymer Nanoparticles via RAFT Aqueous Emulsion Polymerization. A typical protocol for the synthesis of $PMAA_{56}$-$PBzMA_{500}$-$PBMA_{500}$-$PBzMA_{500}$ nanoparticles was as follows. $PMAA_{56}$ macro-CTA (0.1757 g, 0.03 mmol), ACVA (1.9 mg; 0.01 mmol, CTA/initiator molar ratio = 5.0) and water (7.42 g, 30 % w/w) were weighed into a 25 mL round-bottomed flask. The solution pH was adjusted to pH 5 using 1 M NaOH, followed by addition of BzMA monomer (3.00 g, 0.02 mol). A magnetic flea was added and the reaction vial was sealed using a rubber septum. The reaction solution was then purged under N_2 for 20 min before placing the vial in a pre-heated water bath at 70 ^oC for 120 min. A 1.0 mL sample of the diblock copolymer dispersion was removed using a syringe under a N_2 atmosphere. Previously degassed BMA monomer (2.10 g, 0.02 mol) and water (0.85 g, 40 % w/w) were then injected into the vial using a syringe under a N_2 atmosphere. The second-stage polymerization was allowed to proceed for a further 180 min at 70 ^oC. A 1.0 mL sample of the triblock copolymer dispersion was removed using a syringe under a N_2 atmosphere. Previously degassed BzMA monomer (2.24 g, 0.01 mol) and water (1.58 g, 45 % w/w) were then injected into the vial using a syringe under a N_2 atmosphere. The third-stage polymerization was allowed to proceed for a further 18 h at 70 ^oC, before removing the vial from the water bath and exposing its contents to air to quench the reaction.

High-Throughput Syntheses of Diblock Copolymer Nanoparticles via RAFT Aqueous Emulsion Polymerizations using the Chemspeed Autoplant A100. A typical protocol for the synthesis of $PMAA_{56}$-$PBzMA_{500}$ nanoparticles was as follows: Firstly, an aqueous stock solution containing $PMAA_{56}$ macro-CTA (38.3 mg dm^{-3}) and ACVA initiator (0.40 mg dm^{-3}) was prepared and adjusted to pH 5 using 1 M NaOH. Up to twenty reactor vessels were then charged with this stock solution (17.75 g). The monomer (BzMA, 5.12 g) was then added over 10 min, while further water was added (3.95 g) to adjust to the desired overall solids concentration (20 % w/w). A stream of N_2 gas was blown through all the reaction vessels for 20 min. The reaction vessels were then sealed and heated up to 70 ^oC. Each vessel was equipped with an overhead stirrer. Either a propeller-type stirrer (at 350-650 rpm) or an anchor-type stirrer (at 150-350 rpm) was used (see Figure 1). The stirring range used for each stirrer geometry was selected to afford efficient mixing with minimal splashing, as judged by visual inspection. The anchor stirrer generates significantly higher shear rates than the propeller stirrer at an equivalent stirring speed (rpm). All reaction vessels were maintained at 70 ^oC for 1 h before cooling to room temperature and decanting into 100 mL sample bottles. These reactions

were also performed using BMA monomer. Batch sizes for the synthesis of $PMAA_{56}$-$PBzMA_{500}$ and $PMAA_{56}$-$PBMA_{500}$ were ~27 g and ~22 g respectively. In further experiments, these syntheses were also conducted at a higher overall solids concentration of 30 % w/w.

High-Throughput Syntheses of Triblock and Tetrablock Copolymers via RAFT Aqueous Emulsion Polymerization using the Chemspeed Autoplant A100. Initially, the same protocol as that described above for the diblock copolymer syntheses was employed. Then, at the end of the 1 h reaction time, a second water-immiscible monomer (BzMA or BMA) was injected into the reaction solution for the second-stage polymerization. Further water was also added to adjust the overall solids concentration to 40 % w/w. The reaction solution was then held at 70 ^{o}C for 2 h. For the synthesis of tetrablock copolymer nanoparticles (45 % w/w solids), a third water-immiscible monomer (BzMA or BMA) and further water was added after completion of the triblock copolymer synthesis. Each reaction vessel was then held at 70 ^{o}C for 2 h before cooling to room temperature and exposing to air to quench the polymerization.

Instrumentation and Copolymer Characterization

The Chemspeed Autoplant A100 high-throughput robot. This apparatus was equipped with a four-needle head, 10 mini-plant modules and 10 pump modules (see Figure 1). Each mini-plant module can house two 100 mL steel reactors that can be heated and stirred independently as well as connecting to a refluxing 80:20 water/ethanol mixture to allow reactor head cooling. Stirrer blades were available with either anchor or propeller geometries and stirrer speeds could be varied from 50 to 1000 rpm. Heating is controlled by individual electrically-heated jackets around each vessel that can be individually heated from ambient temperature up to 200 °C with valves connected to chilled fluid for cooling. The cooling fluid (silicone oil) is provided by a dynamic temperature control system /circulation thermostat (Huber Unistat Tango). An inert atmosphere was maintained by applying a 1.1 bar flow of N_2 through all the reactors, at a flow rate of 0.8 L min^{-1}. With additional pump modules, the A100 can feed up to three liquid materials to each reactor in parallel. The liquid feeding (dosing) is completed using syringe pumps that are capable of continuous cycles of aspiration and dispensation (one 100 μL syringe and two 50 μL syringes). The software used to control the A100 was 'Chemspeed Autosuite 1.11.2.24'.

^{1}H NMR Spectroscopy. All ^{1}H NMR spectra were recorded using a 400 MHz Bruker Advance-400 spectrometer using d_4-methanol or d_8-tetrahydrofuran as the solvent.

Dynamic Light Scattering (DLS). Aqueous copolymer dispersions (0.20 % w/w) in disposable plastic cuvettes were analyzed at 20 °C using a Malvern Zetasizer NanoZS instrument. Scattered light was detected at 173° and intensity-average hydrodynamic diameters were calculated using the Stokes-Einstein equation. Data were averaged over three consecutive measurements, comprising a minimum of ten runs per measurement. The particle diameter standard deviations were calculated from the DLS polydispersities.

Transmission Electron Microscopy (TEM). Each sample was prepared by depositing 10 µL (0.20 % w/w) of 0.1 % w/w aqueous copolymer dispersion onto a glow-discharged carbon-coated copper grid for 20 seconds. The grid was then stained with 10 µL uranyl formate solution (0.75 % w/w) for 10 seconds and carefully dried using a vacuum hose. TEM images were recorded using a Philips CM100 instrument operating at 100 kV and connected to a Gatan 1 k CCD camera. ImageJ software was used to determine mean nanoparticle diameters from TEM images (at least 100 nanoparticles were analyzed per sample). Standard deviations were calculated using Microsoft Excel.

High-Performance Liquid Chromatography (HPLC) for Monomer Conversion

A stock solution was made up comprising both BzMA (0.100 g) and BMA (0.100 g) dissolved in acetonitrile (100 mL). This stock solution was serially diluted to afford four calibration solutions with concentrations ranging from 5.68 x 10^{-2} mmol dm^{-3} to 1.41 mmol dm^{-3} for BzMA and from 7.03 x 10^{-2} mmol dm^{-3} to 1.41 mmol dm^{-3} for BMA. Samples (0.100 g) were dissolved in acetonitrile (10 mL), before filtering through a 0.45 um filter. The experimental set-up comprised an Agilent 1200 quaternary pump operating at a flow rate of 0.50 mL min^{-1} in series with an Agilent 1200 evaporative light scattering detector maintained at 40 °C, and a diode array variable wavelength UV detector (set to wavelengths of 205 and 254 nm). The eluent was initially 60:40 v/v acetonitrile/water (for 11 min) before being gradually increased to 90:10 v/v acetonitrile/water over 4 min and then held constant for the final 5 min. Linear calibration plots were obtained for both BMA and BzMA monomers using this protocol (see Figure S2).

Gel Permeation Chromatography (GPC). THF GPC was used to determine copolymer molecular weights and dispersities at 30 °C. For analysis of polymers synthesized via the high-throughput protocol the GPC set-up consisted of an autosampler, Viscotex 2001 GPC max pump, PSS SDV analytical pre-column column (10 µm, 50 mm x 8.0 mm), 3 PSS SDV analytical columns (10 µm, 300 mm x 8.0 mm, 1000 Å; 10 µm, 300 mm x 8.0 mm, 10^5 Å; 10 µm, 300 mm x 8.0 mm, 10^7 Å), connected to a Viscotek TDA 305 refractive index detector. For analysis of polymers synthesized on a laboratory-scale the GPC set-up consisted of an

Agilent 1260 Infinity II GPC/SEC system fitted with an autosampler and two 5 μM Mixed-B columns connected to a refractive index detector. In both protocols, the mobile phase was HPLC-grade THF containing 4.0 % v/v glacial acetic acid at a flow rate of 1.0 mL min^{-1}. Molecular weights were calculated using a series of near-monodisperse poly(methyl methacrylate) calibration standards. The $PMAA_{56}$ macro-CTA and the block copolymers synthesized on a laboratory-scale were modified by exhaustive methylation of its carboxylic acid groups to render them THF-soluble. This was achieved by adding excess trimethylsilyldiazomethane dropwise to a solution of copolymer (20 mg) in THF (2.0 mL) until a persistent yellow coloration was observed. This reaction solution was then stirred overnight until all THF had evaporated, prior to GPC analysis.

Results and Discussion

For the RAFT aqueous emulsion polymerization formulations explored in this study, a water-soluble poly(methacrylic acid) macro-CTA was dissolved in water at pH 5 and then chain-extended using a water-immiscible monomer (either BzMA or BMA). This water-immiscible monomer polymerizes to form a water-insoluble polymer, which leads to in situ self-assembly of the propagating diblock copolymer chains to form sterically-stabilized nanoparticles via PISA.[10-28]

Laboratory-scale syntheses of $PMAA_{56}$-$PBzMA_{500}$ diblock copolymer nanoparticles were typically performed on a ~10–11 g scale using 15 mL glass vials. $PMAA_{56}$ macro-CTA, ACVA initiator and water were weighed into each vial and the solution pH was adjusted to pH 5 before addition of BzMA monomer (according to Chaduc and co-workers this pH is optimal for the synthesis of PMAA-containing diblock copolymer nanoparticles via RAFT aqueous emulsion polymerization).[21, 23] The vial was then sealed and degassed in ice by bubbling N_2 through the reaction mixture for 15 min with continuous magnetic stirring at approximately 500 rpm, prior to heating to 70 ^{o}C using an oil bath. In contrast, for the Chemspeed A100 automated synthesizer (Figure 1) each reaction must be performed on a 15 to 80 mL scale and stirred using an overhead mechanical stirring unit (equipped with either an anchor or propeller stirrer). Moreover, for such parallel syntheses it is not feasible to degas reaction mixtures within individual vessels using a N_2 sparge.

Scheme 1. Synthesis of a) $PMAA_{56}$ macro-CTA via RAFT solution polymerization in ethanol and synthesis of b) $PMAA_{56}$-$PBzMA_{500}$ and c) $PMAA_{56}$-$PBMA_{500}$ diblock copolymer nanoparticle via RAFT aqueous emulsion polymerization. These RAFT aqueous emulsion polymerizations were performed at pH 5 at which the $PMAA_{56}$ macro-CTA has an approximate degree of ionization of 11 %.

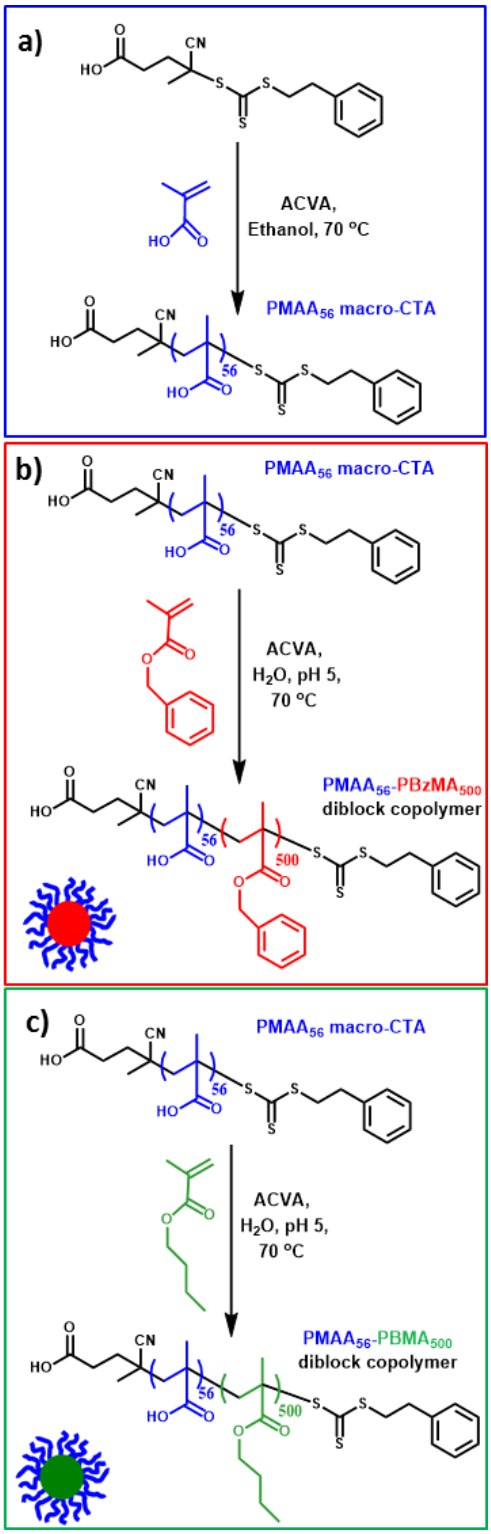

For the successful transfer of such PISA formulations from individual lab-scale syntheses to high-throughput syntheses, three essential differences need to be taken into consideration. Firstly, weighing out four components and adjusting the solution pH in all 20 reaction vessels is simply too time-consuming. Secondly, it is not possible to bubble N_2 through the reaction mixture contained in each of the twenty reaction vessels. Thirdly, using an overhead mechanical stirrer instead of a magnetic flea should enable more efficient stirring, but additional factors such as stirrer geometry may be important.

To avoid weighing out each reagent individually into all twenty reaction vessels, a stock aqueous solution containing the $PMAA_{56}$ macro-CTA, ACVA initiator and water (adjusted to pH 5) was used to charge each reactor vessel. This stock solution comprised $PMAA_{56}$ macro-CTA (38.3 g dm^{-3}) and ACVA (0.40 g dm^{-3}), giving a macro-CTA/initiator molar ratio of 5.0. A predetermined volume of the stock solution (5-20 mL) was injected into each reaction vessel to produce the PISA formulation required for a given target diblock copolymer composition. The monomer was then injected, along with further water (0-25 mL) to adjust the final solids concentration.

RAFT polymerization is a type of reversible deactivation radical polymerization: the use of a highly reactive chain transfer agent creates a rapid and reversible equilibrium between active and dormant polymer chains.[1] If oxygen is present, it can react with the polymer radicals and retard the rate of polymerization.[84, 85] Hence thorough deoxygenation of the reaction solution is required for RAFT polymerizations. This is typically achieved by bubbling N_2 gas directly through the reaction mixture. However, this is not possible with the Chemspeed A100. Instead, N_2 gas was blown through the reaction chamber for 20 min (at 20 °C) while stirring the reaction mixture at 200 rpm prior to initiation of the polymerization. Initial experiments confirmed that this modified protocol provided sufficient protection from aerial oxygen to enable high monomer conversions (> 94 %) to be achieved during RAFT aqueous emulsion polymerization.

In conventional emulsion polymerization, it is well-documented that efficient stirring is of critical importance.[86, 87] Firstly, inefficient stirring can lead to the formation of relatively large monomer droplets which can potentially act as the locus of polymerization. This leads to suspension polymerization, rather than emulsion polymerization. Secondly, the stirring rate

Figure 1. Digital photographs showing (a) the Chemspeed A100 automated synthesizer, (b) a 100 mL reaction vessel and stirrer module, (c) a propeller-type stirrer and (d) an anchor-type stirrer.

may influence both the rate of polymerization and the final particle diameter.[88] Indeed, Charleux and co-workers reported that the stirring rate can have a significant impact on the success of RAFT aqueous emulsion polymerization formulations.[17] Moreover, colloidally stable dispersions could not be obtained in the present study when using unstirred reaction

mixtures in laboratory-scale control experiments, see Figure S3. When using the Chemspeed A100, reaction mixtures were mechanically stirred at 150 to 650 rpm using an overhead stirrer unit with either anchor or propeller stirrers (Figure 1). Ideally, our high-throughput protocol for RAFT aqueous emulsion polymerization should be applicable for a wide range of formulations. Thus, two water-immiscible methacrylic monomers (BzMA and BMA, see Scheme 1) were selected to have differing densities: BzMA is slightly more dense than water (1.04 g cm^{-3} at 25 ^{o}C), whereas BMA is slightly less dense than water (0.89 g cm^{-3} at 25 ^{o}C). Thus the former monomer droplets tend to sediment, whereas the latter tend to cream; ideally, the stirrer type should be able to cope with this difference in droplet buoyancy. A $PMAA_{56}$ macro-CTA was chain-extended using each monomer while targeting a mean core-forming block DP of 500; all reaction conditions were kept constant while evaluating the two stirrer geometries for a range of stirring rates. Each RAFT aqueous emulsion polymerization was conducted on a 15 to 20 mL scale using a propeller stirrer at stirring speeds of 350, 450, 550 and 650 rpm and with an anchor stirrer at stirring speeds of 150, 250 and 350 rpm (see Table 1). For the former stirrer, only the lowest propeller blade was immersed in the reaction mixture, thus mimicking the stirring achieved with a magnetic flea. This set-up provided adequate stirring and enabled more than 98 % conversion to be achieved for both monomers (BzMA and BMA) at all stirring speeds, with both stirrer geometries (see Table 1). The single exception to this was during the synthesis of $PMAA_{56}$-$PBzMA_{500}$ with the anchor stirrer at 350 rpm, where significantly lower conversion (78 %) were observed (see Table 1). Furthermore, GPC analysis indicated that reduced RAFT control was achieved (M_w/M_n = 1.39-1.84) with the anchor stirrer compared to the propeller stirrer (M_w/M_n = 1.36-1.48), see Table 1.

Finally, the GPC data obtained for the laboratory-scale syntheses of these diblock copolymers differ significantly from that obtained from the corresponding high-throughput syntheses, with the latter giving narrower molecular weight distributions (see Table 1 and Figure S4). However, it is worth emphasizing that these two data sets were analyzed using separate GPC instruments with differing column sets. Moreover, the copolymers obtained from the laboratory-scale syntheses were methylated using excess trimethylsilyldiazomethane, whereas those prepared using the high-throughput protocol were not subjected to this chemical derivatization.

Table 1. Summary of the effect of stirrer geometry and stirring rate (rpm) on the synthesis of $PMAA_{56}$-$PBzMA_{500}$ and $PMAA_{56}$-$PBMA_{500}$ diblock copolymer nanoparticles via high-throughput RAFT aqueous emulsion polymerization at 70 ºC. All reactions were performed at 20 % w/w solids using a macro-CTA/initiator molar ratio of 5.0.

Monomer type	Monomer density at 20 ºC (g cm^{-3})	Water solubility at 20 ºC (g dm^{-3})	Scale	Stirrer geometry	Stirring rate (rpm)	Conversion (%)[a]	DLS particle diameter (nm)[b]	DLS PDI[b]	GPC[c]	
									M_n (g mol^{-1})	M_w/M_n
BzMA	1.04	0.19	High-Throughput	Propeller	350	99	39	0.19	57,000	1.38
					450	98	43	0.17	56,500	1.36
					550	99	48	0.16	60,300	1.39
					650	99	48	0.16	59,100	1.40
			High-Throughput	Anchor	150	99	45	0.14	68,900	1.39
					250	99	52	0.14	62,200	1.49
					350	78	61	0.18	39,400	1.47
			Laboratory-Scale	Magnetic flea	500	> 99[d]	51	0.14	82,600	1.73
BMA	0.89	0.20	High-Throughput	Propeller	350	99	45	0.25	57,900	1.36
					450	99	45	0.20	59,900	1.44
					550	99	45	0.18	58,100	1.48
					650	99	45	0.16	58,300	1.46
			High-Throughput	Anchor	150	99	47	0.21	63,800	1.56
					250	99	42	0.18	43,000	1.84
					350	99	45	0.17	57,700	1.47
			Laboratory-Scale	Magnetic flea	500	> 99[d]	37	0.15	50,500	2.01

[a]Final monomer conversion determined by high-performance liquid chromatography (HPLC).
[b]Particle diameter determined by dynamic light scattering (DLS).
[c] Molecular weight data determined by GPC using THF eluent containing 4 % v/v glacial acetic acid (against a series of near-monodisperse poly(methyl methacrylate) standards). The high-throughput and laboratory-scale polymers were analyzed using separate GPC instruments with differing column sets. Moreover, the copolymers obtained from the laboratory-scale syntheses were methylated using excess trimethylsilyldiazomethane, whereas those prepared using the high-throughput protocol were not subjected to this chemical derivatization.

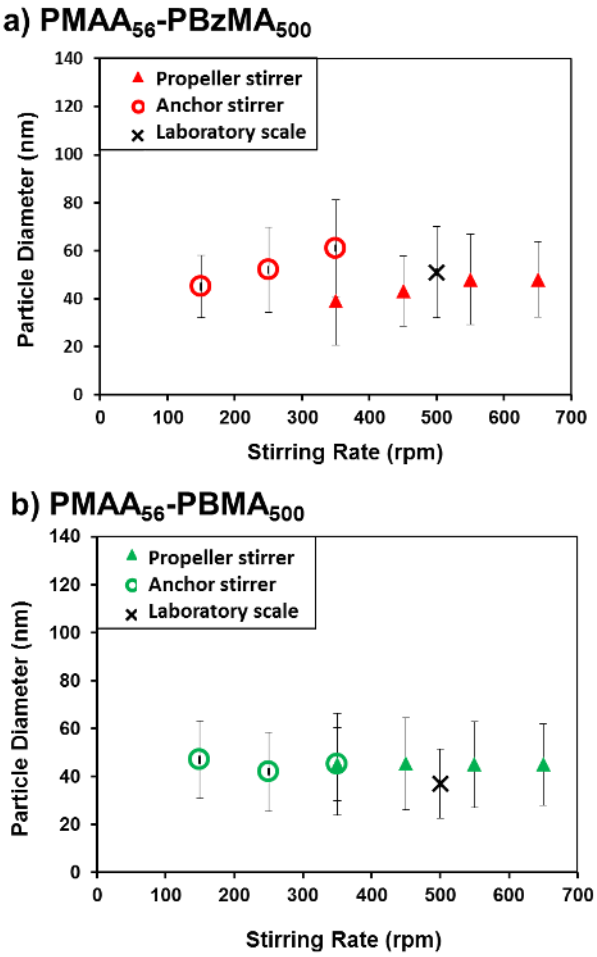

Figure 2. Summary of dynamic light scattering (DLS) data showing the effect of stirrer geometry and stirring rate (rpm) on the intensity-average particle diameter (nm) for (a) $PMAA_{56}$-$PBzMA_{500}$ and (b) $PMAA_{56}$-$PBMA_{500}$ diblock copolymer nanoparticles prepared via high-throughput RAFT aqueous emulsion polymerization using the Chemspeed AutoPlant A100 synthesizer. Filled triangles indicate syntheses conducted using the propeller stirrer, open circles indicate syntheses performed using the anchor stirrer and crosses indicate laboratory-scale syntheses. Error bars indicate the standard deviations for each particle size distribution, rather than the experimental error.

For the BzMA polymerizations, some variation in the intensity-average diameter was observed when adjusting the stirring rate for both stirrer geometries (Figure 2 and Figure S5). When using the anchor stirrer, a modest increase in nanoparticle diameter from 45 to 61 nm was observed as the stirring rate was increased from 150 to 350 rpm. A smaller increase in nanoparticle diameter (from 39 to 45 nm) with stirring rate was observed for polymerizations using the propeller stirrer. In contrast, the stirrer geometry and stirring rate had minimal effect on the intensity-average diameter for BMA polymerizations (Figure 2 and Figure S4). In addition, the particle size was comparable to those achieved during laboratory scale syntheses of the $PMAA_{56}$-$PBzMA_{500}$ and $PMAA_{56}$-$PBMA_{500}$ diblock copolymer nanoparticles (which afforded intensity-average diameters of 51 nm and 37 nm, respectively). Overall, it seems that the propeller stirrer provides more effective stirring than the anchor stirrer for these RAFT

aqueous emulsion polymerizations and that the monomer density has little influence on the formation of monomer droplets under shear.

The reproducibility of such high-throughput syntheses using the Chemspeed A100 was then evaluated by preparing both $PMAA_{56}$-$PBzMA_{500}$ and $PMAA_{56}$-$PBMA_{500}$ nanoparticles five times using precisely the same formulation in each case. These formulations were conducted in randomized locations on the Chemspeed A100. The resulting diblock copolymer dispersions were then analyzed by HPLC, DLS and TEM for comparison, along with THF GPC analyses of the copolymer chains (see Table 2). All five $PMAA_{56}$-$PBzMA_{500}$ syntheses proceeded to high conversion within 1 h (> 98 %) while GPC analyses indicated comparable molecular

Table 2. Assessment of the reproducibility of the PISA synthesis of diblock copolymer nanoparticles via high-throughput RAFT aqueous emulsion polymerization of either benzyl methacrylate (BzMA) or n-butyl methacrylate (BMA) at 70 °C using a $PMAA_{56}$ macro-CTA at pH 5.

Monomer type	Experiment number	Conversion (%)[a]	DLS particle diameter (nm)[b]	DLS PDI[b]	TEM particle diameter (nm)[c]	M_n (g mol^{-1})[d]	M_w/M_n
BzMA	1	99	44	0.15	31	56, 900	1.57
	2	99	46	0.14	31	58, 400	1.55
	3	98	45	0.13	31	57, 300	1.49
	4	99	45	0.14	34	58, 000	1.50
	5	99	45	0.14	34	57, 700	1.48
BMA	1	98	45	0.20	33	51,300	1.67
	2	98	43	0.18	37	50, 300	1.62
	3	98	43	0.16	36	55, 900	1.54
	4	98	45	0.16	34	53, 100	1.60
	5	98	46	0.18	35	54, 600	1.60

[a] Conversion determined by high-performance liquid chromatography (HPLC)
[b] Intensity-average particle diameter determined by dynamic light scattering (DLS)
[c] Number-average particle diameter determined by transmission electron microscopy (TEM)
[d] Molecular weight data determined by GPC using THF eluent containing 4 % v/v glacial acetic acid (calibrated using a series of near-monodisperse poly(methyl methacrylate) standards).

weight distributions in each case (M_n = 56 700 ± 500 g mol^{-1} and M_w/M_n = 1.48-1.57) (Figure 3a). Similarly, each of the five $PMAA_{56}$-$PBMA_{500}$ syntheses proceeded to 98 % conversion within 1 h (M_n = 53 400 ± 2 100 g mol^{-1} and M_w/M_n =1.54-1.67, Figure 3b). THF GPC chromatograms also confirm high blocking efficiencies and unimodal traces in all cases. Moreover, there was generally minimal variation in the intensity-average particle diameter between the $PMAA_{56}$-$PBzMA_{500}$ series (44 nm to 46 nm) and the $PMAA_{56}$-$PBMA_{500}$ series (43 to 46 nm), see Figure 4 and Figure S6. However, TEM analysis (which is only sensitive to the nanoparticle cores, and so underestimates relative to the hydrodynamic diameter reported by DLS) indicated the formation of spherical nanoparticles with comparable particle diameters in all cases, see Figure 5.

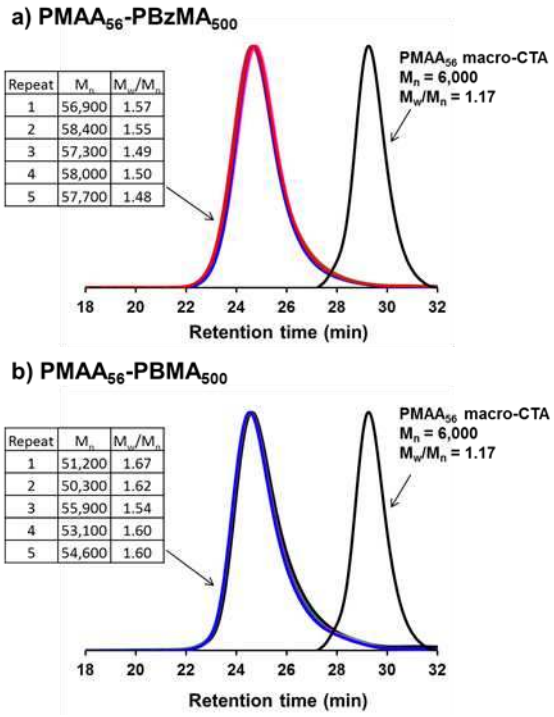

Figure 3. THF GPC chromatograms confirm that good reproducibility is achieved for molecular weight distributions when targeting (a) $PMAA_{56}$-$PBzMA_{500}$ and (b) $PMAA_{56}$-$PBMA_{500}$ nanoparticles via high-throughput RAFT aqueous emulsion polymerizations performed using the Chemspeed A100. Each synthesis was conducted five times and the corresponding chromatograms are overlaid. Tables summarize the M_n and M_w/M_n data calculated from each chromatogram.

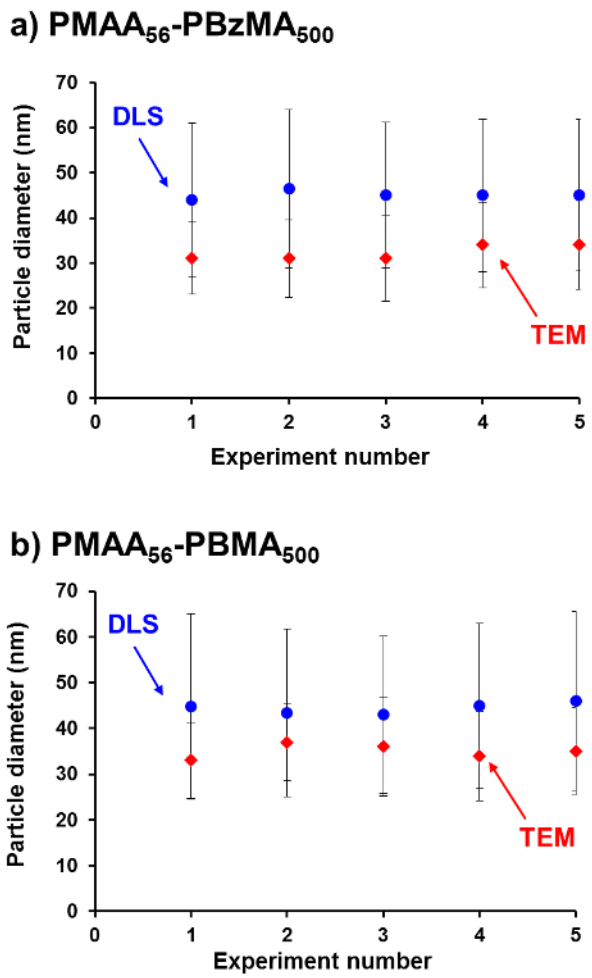

Figure 4. Particle size analysis of diblock copolymer nanoparticles synthesized via high-throughput RAFT aqueous emulsion polymerization using the Chemspeed Autoplant A100 automated synthesizer: (a) $PMAA_{56}$-$PBzMA_{500}$ and (b) $PMAA_{56}$-$PBMA_{500}$. Particle diameter as measured by DLS (blue circles) and by TEM (red diamonds). Error bars indicate standard deviations for each particle size distribution, rather than the experimental error.

In summary, the observed minimal variation in conversion, molecular weight, dispersity and mean particle diameter indicate rather good reproducibility for the high-throughput RAFT aqueous emulsion polymerizations performed using the Chemspeed A100.

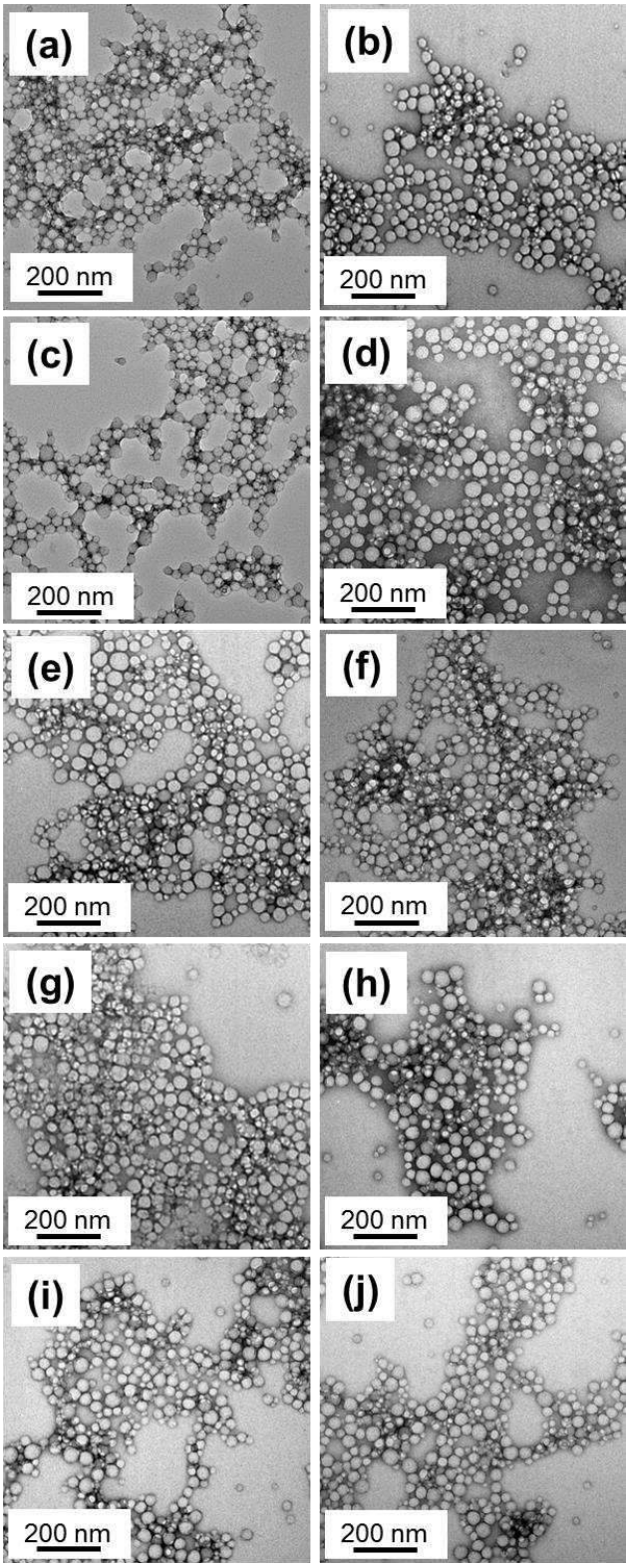

Figure 5. Representative TEM images of diblock copolymer nanoparticles synthesized via high-throughput RAFT aqueous emulsion polymerization using the Chemspeed Autoplant A100 automated synthesizer: (a-e) $PMAA_{56}$-$PBzMA_{500}$ and (f-j) $PMAA_{56}$-$PBMA_{500}$.

Having demonstrated reproducible RAFT aqueous emulsion polymerization syntheses for both $PMAA_{56}$-$PBzMA_{500}$ and $PMAA_{56}$-$PBMA_{500}$ nanoparticles, the versatility of this optimized high-throughput approach was assessed for the synthesis of methacrylic-based multiblock nanoparticles.[89] In a third series of experiments, various triblock and tetrablock copolymer nanoparticles were prepared via a one-pot protocol using sequential monomer addition. In this case, the same $PMAA_{56}$ macro-CTA was chain-extended with BzMA, followed by BMA and then (in the case of the tetrablocks) BzMA, with a target DP of 500 for each block (Scheme 2, Route A). The sequence of the two core-forming blocks was then reversed; the $PMAA_{56}$ macro-CTA was chain-extended first with BMA, followed by BzMA and finally with BMA (see Scheme 2, Route B). These PISA syntheses were completed within 3 h in the case of the triblock copolymer nanoparticles (40 % w/w solids; > 99 % overall conversion), see Table S1 and Figure S6. However, tetrablocks (45 % w/w solids) suffer from incomplete conversions (87-96 % within 5 h) and hence most likely represent the upper limit for this approach, see Table S1 and Figure S7.

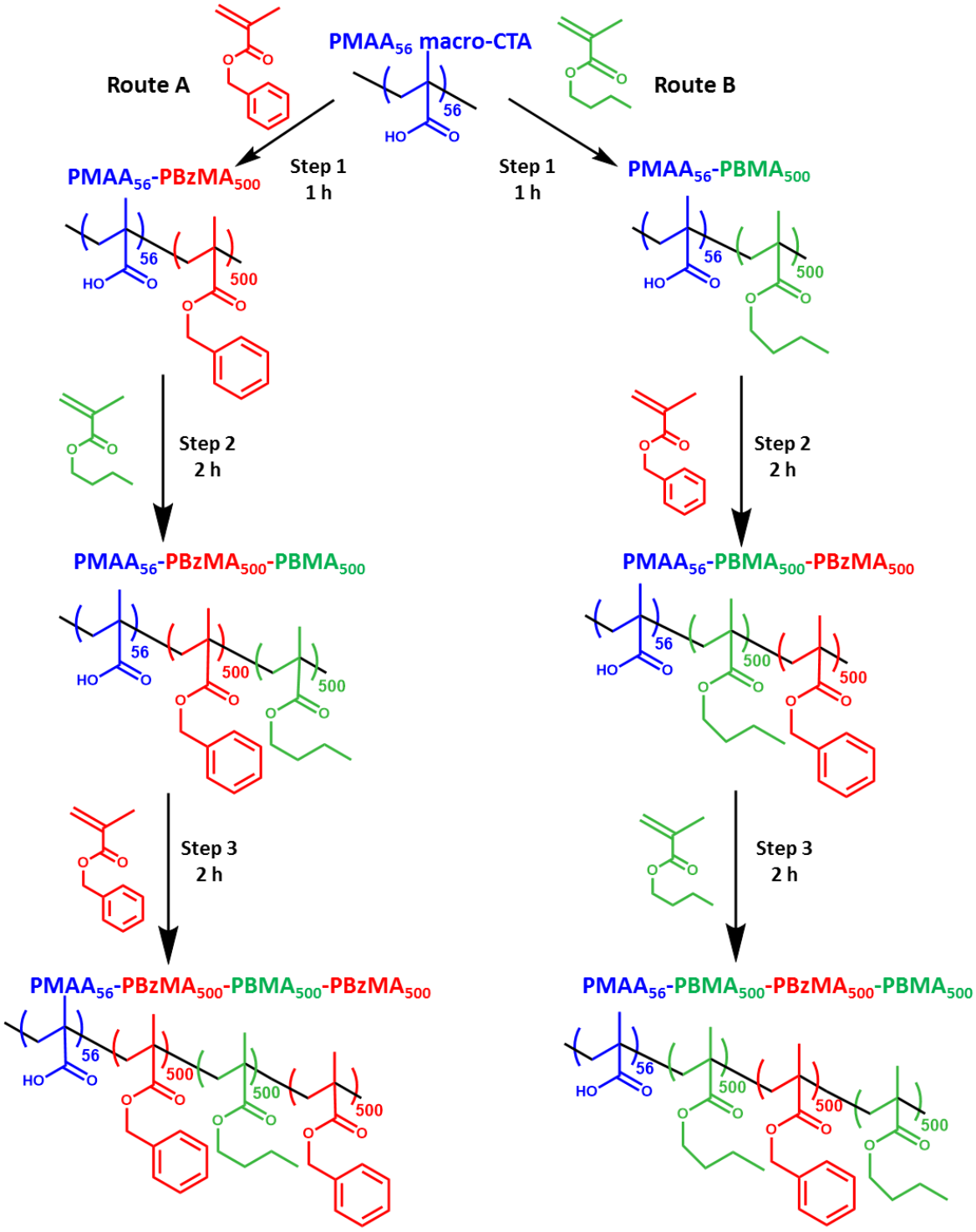

Scheme 2. Synthesis of diblock, triblock and tetrablock copolymers prepared via high-throughput RAFT aqueous emulsion polymerization using the Chemspeed A100 robot synthesizer. A $PMAA_{56}$ macro-CTA was chain-extended with BzMA, followed by BMA and then (in the case of the tetrablocks) BzMA, with each insoluble block having a target DP of 500. The sequence of the two core-forming blocks was also reversed; thus the $PMAA_{56}$ macro-CTA was chain-extended first with BMA, followed by BzMA and then BMA. These multiblock syntheses were performed at 70 °C using a $PMAA_{56}$ macro-CTA/initiator of 5.0, in aqueous solution at pH 5. A propeller stirrer was used at 700 rpm for Step 1 and at 900 rpm for Step 2 and 3.

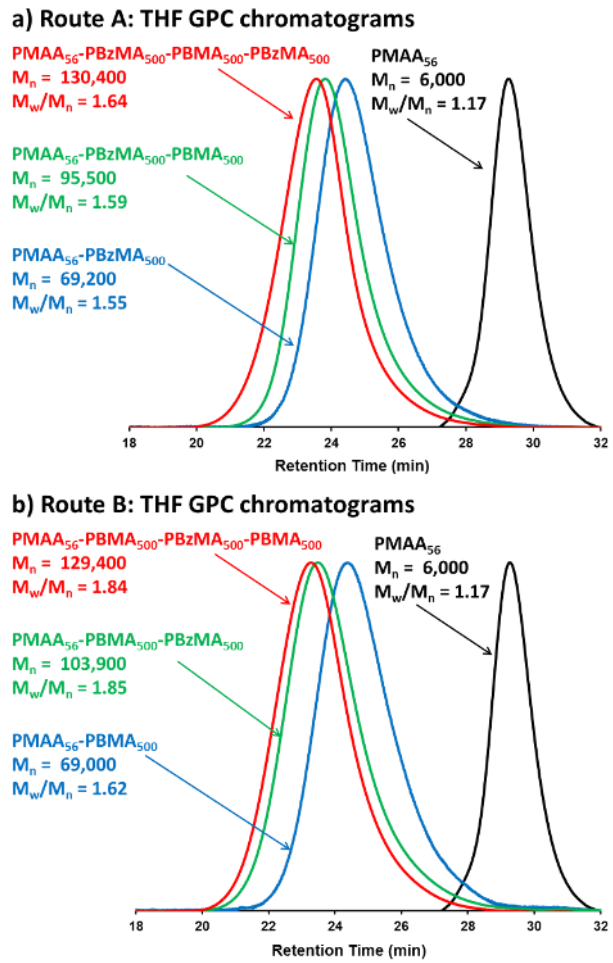

Figure 6. THF GPC chromatograms illustrating the monotonic increase in block copolymer molecular weight achieved with each subsequent block addition during the high-throughput synthesis of diblock, triblock and tetrablock copolymer nanoparticles by RAFT aqueous emulsion polymerization using the Chemspeed A100. All M_n values are expressed relative to poly(methyl methacrylate) calibration standards.

THF GPC analysis indicated a progressive increase in molecular weight during the synthesis of the tetrablock copolymer, see Figure 6. Clearly, the M_w/M_n values obtained throughout this study (M_w/M_n = 1.35 to 1.85) are generally higher than those normally reported for RAFT aqueous emulsion polymerization syntheses. However, there are a number of literature reports that also report relatively broad molecular weight distributions for such PISA formulations.[16-18, 22, 23, 26] Frankly, we are not sure why relatively high M_w/M_n values are observed in the present studies. Nevertheless, the GPC data shown in Figure 6 indicate unimodal distributions and high blocking efficiencies. Thus well-defined, albeit relatively polydisperse, block copolymers are obtained with minimal macro-CTA contamination. In summary, RAFT control is admittedly imperfect in these PISA syntheses, but it is emphasized that there is no evidence for the premature loss of chain-end functionality from the precursor poly(methacrylic acid) block, which would otherwise result in bimodal molecular weight distributions.

Finally, the GPC data obtained for the laboratory-scale synthesis of the tetrablock copolymers differ significantly from that obtained from the corresponding high-throughput syntheses, with the former giving broader molecular weight distributions (compare Figure S8 and Figure 6). However, such discrepancies may well be attributable to differing GPC analytical protocols and instrument set-ups, as noted earlier.

TEM and DLS studies confirmed that colloidally stable spherical nanoparticles were obtained in all cases (see Figure 7, Figure S9 and Figure S10). Owing to the larger (~30 mL) scale and higher solids concentrations (30-45% w/w) used for these reactions, the stirring rate was raised to 700 rpm for the diblock copolymer syntheses and to 900 rpm for the triblock and tetrablock syntheses.

In summary, RAFT aqueous emulsion polymerization can be used for the synthesis of methacrylic tetrablock nanoparticles at up to 45% w/w solids within 5 h, which is comparable to industrial latex formulations based on conventional emulsion polymerization. However, the latter technique cannot be used to access diblock copolymer architectures, so RAFT aqueous emulsion polymerization may offer new potential applications in terms of nanoscale phase separation.

Conclusions

We report optimized protocols for performing high-throughput RAFT aqueous emulsion polymerizations using a commercial automated robot synthesizer (Chemspeed A100). In addition to thorough deoxygenation of the reaction solution, reproducible formulations required using a propeller-type stirrer at stirring rates of 550-900 rpm to produce sufficiently small droplets of the water-immiscible benzyl methacrylate or n-butyl methacrylate monomer. Various sterically-stabilized diblock copolymer nanoparticles could be prepared with final monomer conversions of ≥ 95 % within 1 h. GPC studies indicated very high blocking efficiencies but relatively broad molecular weight distributions ($M_w/M_n \leq 1.70$). TEM studies confirm that a well-defined spherical morphology was obtained in each case but DLS analyses indicated relatively broad size distributions. A library of various triblock and tetrablock copolymer nanoparticles were also prepared via a convenient one-pot protocol using sequential monomer addition. For the tetrablock copolymers, these latter PISA syntheses led to final conversions of 87-96 % within 5 h at 70 °C and good colloidal stability being achieved even at 45 % w/w solids. GPC studies indicate high blocking efficiencies but relatively broad molecular weight distributions (M_w/M_n = 1.36-1.85), suggesting well-defined (albeit rather polydisperse) block copolymers. These preliminary studies provide the basis for further high-

throughput screening of RAFT-mediated PISA formulations, which is likely to be required for commercialization of this promising technology.

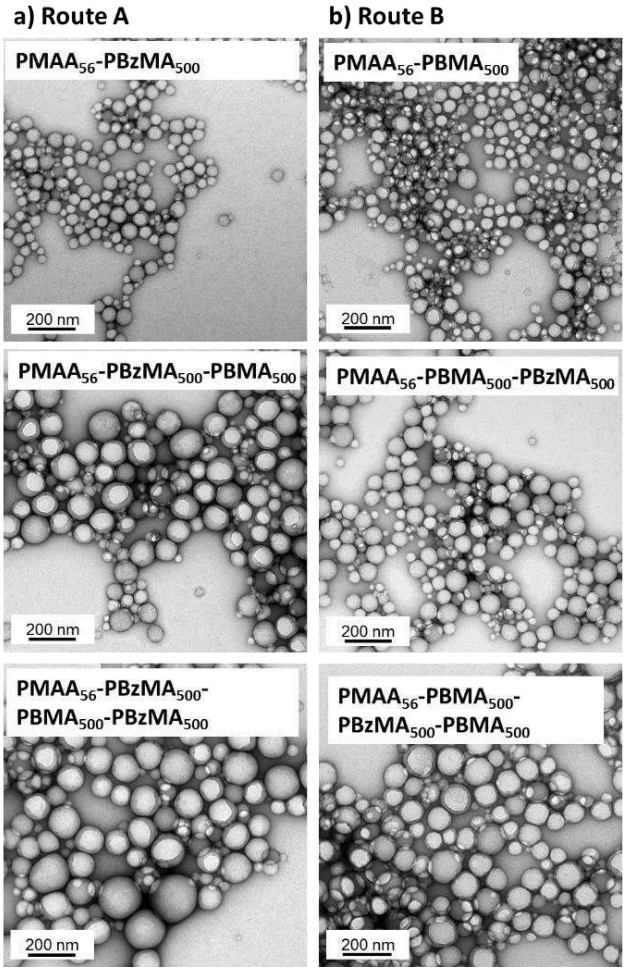

Figure 7. Representative TEM images obtained for the synthesis of diblock, triblock and tetrablock copolymers using the Chemspeed A100 automated synthesizer by RAFT aqueous emulsion polymerization. Spherical morphologies were obtained in all cases and an increase in mean nanoparticle diameter was observed by DLS and TEM with each subsequent block addition.

Author Information

Corresponding Author

*E-mail s.p.armes@sheffield.ac.uk (S.P.A.)

ORCID

Steven P. Armes: 000-0002-8289-6351

Amy A. Cockram: 0000-0002-2289-4389

Acknowledgments

EPSRC and AkzoNobel (Slough, UK) are thanked for funding a CDT PhD CASE studentship for A.A.C. (EP/L016281/1). In addition, S.P.A. acknowledges an ERC Advanced Investigator grant (PISA 320372). The authors are grateful to AkzoNobel for hosting A.A.C. during a six-month placement at their Slough site, where most of this work was conducted. D. Anand, S. Javed, K. Erdelyi-Brooks and D. Sanjuan are thanked for their technical advice regarding the polymer syntheses. J. Pricopi performed all HPLC analyses and A. Szczygiel, S. Murray, D. Pearce, A. Robinson and C. Baldassarri are acknowledged for their assistance and advice regarding the NMR, GPC and TEM studies. AkzoNobel is also thanked for permission to publish this work.

References

1. J. Chiefari, Y. K. B. Chong, F. Ercole, J. Krstina, J. Jeffery, T. P. T. Le, R. T. A. Mayadunne, G. F. Meijs, C. L. Moad, G. Moad, E. Rizzardo and S. H. Thang, Macromolecules, 1998, **31**, 5559-5562.
2. S. Perrier, Macromolecules, 2017, **50**, 7433-7447.
3. M. Semsarilar and S. Perrier, Nature Chemistry, 2010, **2**, 811-820.
4. Y. Mitsukami, M. S. Donovan, A. B. Lowe and C. L. McCormick, Macromolecules, 2001, **34**, 2248-2256.
5. M. S. Donovan, B. S. Sumerlin, A. B. Lowe and C. L. McCormick, Macromolecules, 2002, **35**, 8663-8666.
6. C. L. McCormick and A. B. Lowe, Accounts of Chemical Research, 2004, **37**, 312-325.
7. A. B. Lowe and C. L. McCormick, Progress in Polymer Science, 2007, **32**, 283-351.
8. C. L. McCormick, B. S. Sumerlin, B. S. Lokitz and J. E. Stempka, Soft Matter, 2008, **4**, 1760-1773.
9. A. York, S. Kirkland and C. McCormick, Advanced Drug Delivery Reviews, 2008, **60**, 1018-1036.
10. S. W. Prescott, M. J. Ballard, E. Rizzardo and R. G. Gilbert, Aust. J. Chem, 2002, **55**, 415.
11. C. J. Ferguson, R. J. Hughes, B. T. T. Pham, B. S. Hawkett, R. G. Gilbert, A. K. Serelis and C. H. Such, Macromolecules, 2002, **35**, 9243-9245.
12. C. J. Ferguson, R. J. Hughes, D. Nguyen, B. T. T. Pham, R. G. Gilbert, A. K. Serelis, C. H. Such and B. S. Hawkett, Macromolecules, 2005, **38**, 2191-2204.
13. S. Fréal-Saison, M. Save, C. Bui, B. Charleux and S. Magnet, Macromolecules, 2006, **39**, 8632-8638.
14. M. Manguian, M. Save and B. Charleux, Macromolecular Rapid Communications, 2006, **27**, 399-404.
15. M. F. Cunningham, Progress in Polymer Science, 2008, **33**, 365.
16. S. Boissé, J. Rieger, K. Belal, A. Di-Cicco, P. Beaunier, M.-H. Li and B. Charleux, Chemical Communications, 2010, **46**, 1950-1952.
17. S. Boissé, J. Rieger, G. Pembouong, P. Beaunier and B. Charleux, Journal of Polymer Science Part A: Polymer Chemistry, 2011, **49**, 3346-3354.

18. X. Zhang, S. Boissé, W. Zhang, P. Beaunier, F. D'Agosto, J. Rieger and B. Charleux, Macromolecules, 2011, **44**, 4149-4158.
19. W. Zhang, F. D'Agosto, O. Boyron, J. Rieger and B. Charleux, Macromolecules, 2011, **44**, 7584-7593.
20. I. Chaduc, W. Zhang, J. Rieger, M. Lansalot, F. D'Agosto and B. Charleux, Macromolecular Rapid Communications, 2011, **32**, 1270-1276.
21. I. Chaduc, M. Girod, R. Antoine, B. Charleux, F. D'Agosto and M. Lansalot, Macromolecules, 2012, **45**, 5881-5893.
22. W. Zhang, F. D'Agosto, O. Boyron, J. Rieger and B. Charleux, Macromolecules, 2012, **45**, 4075.
23. I. Chaduc, A. Crepet, O. Boyron, B. Charleux, F. D'Agosto and M. Lansalot, Macromolecules, 2013, **46**, 6013-6023.
24. W. Zhang, F. D'Agosto, P.-Y. Dugas, J. Rieger and B. Charleux, Polymer, 2013, **54**, 2011-2019.
25. V. J. Cunningham, A. M. Alswieleh, K. L. Thompson, M. Williams, G. J. Leggett, S. P. Armes and O. M. Musa, Macromolecules, 2014, **47**, 5613-5623.
26. N. P. Truong, M. V. Dussert, M. R. Whittaker, J. F. Quinn and T. P. Davis, Polym. Chem., 2015, **6**, 3865-3874.
27. J. Lesage de la Haye, X. Zhang, I. Chaduc, F. Brunel, M. Lansalot and F. D'Agosto, Angewandte Chemie International Edition, 2016, **55**, 3739-3743.
28. A. A. Cockram, T. J. Neal, M. J. Derry, O. O. Mykhaylyk, N. S. J. Williams, M. W. Murray, S. N. Emmett and S. P. Armes, Macromolecules, 2017, **50**, 796-802.
29. M. Save, Y. Guillaneuf and R. G. Gilbert, Aust. J. Chem, 2006, **59**, 693-711.
30. Z. An, Q. Shi, W. Tang, C.-K. Tsung, C. J. Hawker and G. D. Stucky, J Am Chem Soc, 2007, **129**, 14493-14499.
31. Y. Li and S. P. Armes, Angewandte Chemie International Edition, 2010, **49**, 4042-4046.
32. A. Blanazs, J. Madsen, G. Battaglia, A. J. Ryan and S. P. Armes, Journal of the American Chemical Society, 2011, **133**, 16581-16587.
33. S. Sugihara, A. Blanazs, S. P. Armes, A. J. Ryan and A. L. Lewis, Journal of the American Chemical Society, 2011, **133**, 15707-15713.
34. W. Shen, Y. Chang, G. Liu, H. Wang, A. Cao and Z. An, Macromolecules, 2011, **44**, 2524-2530.
35. G. Liu, Q. Qiu, W. Shen and Z. An, Macromolecules, 2011, **44**, 5237-5245.
36. A. Blanazs, A. J. Ryan and S. P. Armes, Macromolecules, 2012, **45**, 5099-5107.
37. M. Semsarilar, V. Ladmiral, A. Blanazs and S. P. Armes, Langmuir, 2012, **28**, 914.
38. P. Chambon, A. Blanazs, G. Battaglia and S. P. Armes, Macromolecules, 2012, **45**, 5081.
39. L. P. D. Ratcliffe, A. J. Ryan and S. P. Armes, Macromolecules, 2013, **46**, 769-777.
40. M. Semsarilar, V. Ladmiral, A. Blanazs and S. P. Armes, Langmuir, 2013, **29**, 7416.
41. N. J. Warren and S. P. Armes, Journal of the American Chemical Society, 2014, **136**, 10174-10185.
42. N. J. Warren, O. O. Mykhaylyk, D. Mahmood, A. J. Ryan and S. P. Armes, Journal of the American Chemical Society, 2014, **136**, 1023.
43. J. Rieger, Macromolecular Rapid Communications, 2015, **36**, 1458-1471.
44. B. Charleux, G. Delaittre, J. Rieger and F. D'Agosto, Macromolecules, 2012, **45**, 6753-6765.
45. S. L. Canning, G. N. Smith and S. P. Armes, Macromolecules, 2016, **49**, 1985-2001.
46. J.-T. Sun, C.-Y. Hong and C.-Y. Pan, Soft Matter, 2012, **8**, 7753.
47. J.-T. Sun, C.-Y. Hong and C.-Y. Pan, Polym. Chem., 2013, **4**, 873-881.

48. M. R. Hill, R. N. Carmean and B. S. Sumerlin, Macromolecules, 2015, **48**, 5459-5469.
49. M. J. Derry, L. A. Fielding and S. P. Armes, Progress in Polymer Science, 2016, **52**, 1-18.
50. M. Semsarilar, E. R. Jones, A. Blanazs and S. P. Armes, Advanced Materials, 2012, **24**, 3378-3382.
51. B. Akpinar, L. A. Fielding, V. J. Cunningham, Y. Ning, O. O. Mykhaylyk, P. W. Fowler and S. P. Armes, Macromolecules, 2016, **49**, 5160-5171.
52. A. Blanazs, R. Verber, O. O. Mykhaylyk, A. J. Ryan, J. Z. Heath, C. W. I. Douglas and S. P. Armes, Journal of the American Chemical Society, 2012, **134**, 9741-9748.
53. C. Gonzato, M. Semsarilar, E. R. Jones, F. Li, G. J. P. Krooshof, P. Wyman, O. O. Mykhaylyk, R. Tuinier and S. P. Armes, Journal of the American Chemical Society, 2014, **136**, 11100.
54. N. J. W. Penfold, Y. Ning, P. Verstraete, J. Smets and S. P. Armes, Chemical Science, 2016, **7**, 6894-6904.
55. I. Canton, N. J. Warren, A. Chahal, K. Amps, A. Wood, R. Weightman, E. Wang, H. Moore and S. P. Armes, ACS Central Science, 2016, **2**, 65-74.
56. K. L. Thompson, C. J. Mable, A. Cockram, N. J. Warren, V. J. Cunningham, E. R. Jones, R. Verber and S. P. Armes, Soft Matter, 2014, **10**, 8615.
57. M. J. Rymaruk, K. L. Thompson, M. J. Derry, N. J. Warren, L. P. D. Ratcliffe, C. N. Williams, S. L. Brown and S. P. Armes, Nanoscale, 2016, **8**, 14497-14506.
58. M. Chenal, J. Rieger, C. Véchambre, J.-M. Chenal, L. Chazeau, C. Creton and L. Bouteiller, Macromolecular Rapid Communications, 2013, **34**, 1524-1529.
59. M. Chenal, C. Véchambre, J.-M. Chenal, L. Chazeau, V. Humblot, L. Bouteiller, C. Creton and J. Rieger, Polymer, 2017, **109**, 187-196.
60. L. D. Blackman, K. E. B. Doncom, M. I. Gibson and R. K. O'Reilly, Polymer Chemistry, 2017, **8**, 2860-2871.
61. M. Williams, N. J. W. Penfold, J. R. Lovett, N. J. Warren, C. W. I. Douglas, N. Doroshenko, P. Verstraete, J. Smets and S. P. Armes, Polymer Chemistry, 2016, **7**, 3864-3873.
62. R. Hoogenboom, M. A. R. Meier and U. S. Schubert, Macromol. Rapid Commun., 2003, **24**, 15-32.
63. H. E. Tuinstra and C. H. Cummins, Advanced Materials, 2000, **23**, 1819-1822.
64. M. A. R. Meier, R. Hoogenboom and U. S. Schubert, Macromolecular Rapid Communications, 2004, **25**, 21-33.
65. S. P. Rohrer, E. T. Birzin, R. T. Mosley, S. C. Berk, S. M. Hutchins, D.-M. Shen, Y. Xiong, E. C. Hayes, R. M. Parmar, F. Foor, S. W. Mitra, S. J. Degrado, M. Shu, J. M. Klopp, S.-J. Cai, A. Blake, W. W. S. Chan, A. Pasternak, L. Yang, A. A. Patchett, R. G. Smith, K. T. Chapman and J. M. Schaeffer, Science, 1998, **282**, 737-740.
66. K. C. Nicolaou, A. J. Roecker, S. Barluenga, J. A. Pfefferkorn and G.-Q. Cao, Chem Bio Chem, 2001, **2**, 460-465.
67. B. Jandeleit, D. J. Schaefer, T. S. Powers, H. W. Turner and W. H. Weinberg, Science, 1999, **268**, 1738-1740.
68. X. D. Xiang, X.-D. Sun, G. Briceno, Y. Lou, K.-A. Wang, H. Chang, W. G. Wallace-Freedman, S.-W. Chen and P. G. Schultz, Science, 1995, **268**, 1738-1740.
69. E. Danielson, J. H. Golden, E. W. McFarland, C. M. Reaves, W. H. Weinberg and X. D. Wu, Angewandte Chemie International Edition, 1997, **38**, 2494-2532.
70. X.-D. Sun, C. Gao, J. Wang and X. D. Xiang, Applied Physics Letters, 1997, **70**, 3353-3355.

71. J. Wang, Y. Yoo, C. Gao, I. Takeuchi, X.-D. Sun, H. Chang, X.-D. Xiang and P. G. Schultz, Science, 1998, **279**, 1712-1714.
72. P. G. Schultz and X.-D. Xiang, Current Opinion in Solid State and Materials Science, 1998, **3**, 153-158.
73. S. M. Senkan, Angewandte Chemie International Edition, 1998, **40**, 284-310.
74. M. T. Reetz, Nature, 1998, **394**, 350-353.
75. T. R. Boussie, G. M. Diamond, C. Goh, K. A. Hall, A. M. LaPointe, M. Leclerc, C. Lund, V. Murphy, J. A. W. Shoemaker, U. Tracht, H. Turner, J. Zhang, T. Uno, R. K. Rosen and J. C. Stevens, J Am Chem Soc, 2003, **125**, 4306-4317.
76. T. R. Boussie, G. M. Diamond, C. Goh, K. A. Hall, A. M. LaPointe, M. K. Leclerc, V. Murphy, J. A. W. Shoemaker, H. Turner, R. K. Rosen, J. C. Stevens, F. Alfano, V. Busico, R. Cipullo and G. Talarico, Angewandte Chemie International Edition, 2006, **45**, 3278-3283.
77. P. Chapon, M. Catherine, L. Gilda and D. Mathias, Macromol. Rapid Commun., 2003, **24**, 87-91.
78. M. W. M. Fijten, M. A. R. Meier, R. Hoogenboom and U. S. Schubert, Journal of Polymer Science Part A: Polymer Chemistry, 2004, **42**, 5775-5783.
79. M. W. M. Fijten, R. M. Paulus and U. S. Schubert, Journal of Polymer Science Part A: Polymer Chemistry, 2005, **43**, 3831-3839.
80. R. Hoogenboom and U. S. Schubert, Macromolecules, 2005, **38**, 7653-7659.
81. C. R. Becer, A. M. Groth, R. Hoogenboom, R. M. Paulus and U. S. Schubert, QSAR & Combinatorial Science, 2008, **27**, 977-983.
82. S. Boissé, J. Rieger, G. Pembouong, P. Beaunier and B. Charleux, Journal of Polymer Science Part A: Polymer Chemistry, 2011, **49**, 3346.
83. M. Semsarilar, V. Ladmiral, A. Blanazs and S. P. Armes, Polymer Chemistry, 2014, **5**, 3466-3475.
84. F. A. Bovey and I. M. Kolthoff, Chemical Reviews, 1948, **42**, 491-525.
85. V. A. Bhanu and K. Kishore, Chemical Reviews, 1991, **91**, 99-115.
86. J. W. Goodwin, J. Hearn, C. C. Ho and R. H. Ottewill, Colloid and Polymer Science, 1974, **252**, 464-471.
87. S. Fathi Roudsari, R. Dhib and F. Ein-Mozaffari, Polymer Engineering & Science, 2015, **55**, 945-956.
88. K. Matyjaszewski and T. Davis, Handbook of Radical Polymerization, Wiley, 2002.
89. There has been considerable recent interest in the synthesis of multiblock copolymers via living radical polymerization in the literature (e.g. G. Gody, T. Maschmeyer, P. B. Zetterlund and S. Perrier, Macromolecules, 2014, **47**, 3451-3460 and N. G. Engelis, A. Anastasaki, G. Nurumbetov, N. P. Truong, V. Nikolaou, A. Shegiwal, M. R. Whittaker, T. P. Davis and D. M. Haddleton, Nature Chemistry, 2017, **9**, 171-178).